Absorption spectrum of deuterated water vapor enriched by ^{18}O between 6000 and 9200 cm^{-1}

S.N. Mikhailenko [a,*], O.V. Naumenko [a], A.V. Nikitin [a], I.A. Vasilenko [a], A.-W. Liu [b,**], K.-F. Song [b], H.-Y. Ni [b], S.-M. Hu [b]

[a] Laboratory of Theoretical Spectroscopy, V.E. Zuev Institute of Atmospheric Optics, SB RAS, 1, Akademician Zuev Square, 634021 Tomsk, Russia
[b] Hefei National Laboratory for Physical Sciences at Microscale, University of Science and Technology of China, Hefei 230026, China

A B S T R A C T

The absorption spectrum of water vapor enriched by deuterium and oxygen-18 is analyzed in the 6000–9200 cm^{-1} region. The spectrum has been recorded at room temperature with a Bruker IFS 120 h Fourier transform spectrometer. More than 14,000 absorption lines were measured in the recorded spectrum. The vibration–rotation assignments were performed on the basis of previously published experimental energies and of variational calculations. Nine water species ($H_2^{16}O$, $HD^{16}O$, $D_2^{16}O$, $H_2^{18}O$, $HD^{18}O$, $D_2^{18}O$, $H_2^{17}O$, $HD^{17}O$ and $D_2^{17}O$) were found to contribute to the observed absorption. More than 3600 lines of 19 vibrational bands of $D_2^{18}O$ and about 4700 lines of 16 bands of $HD^{18}O$ with J as high as 19 and K_a as high as 11 were assigned. The main part of the $HD^{18}O$ and $D_2^{18}O$ lines and all lines of $HD^{17}O$ and $D_2^{17}O$ were observed in the laboratory for the first time. The obtained vibration–rotation energy levels are compared with previous experimental studies and the results of variational calculations.

1. Introduction

Water vapor plays a key role in the understanding of the radiative budget of the Earth's atmosphere. The isotope composition of atmospheric water may vary relatively widely from the standard (deep offshore ocean) water due to depletion in heavier isotopologues in the process of evaporation to the atmosphere and condensation from the atmosphere. This depletion provides an integrated history of condensation and evaporation, which helps studying the hydrological cycle. Hence, the information of the vibration–rotation spectra of rare water isotopic species is of importance for atmospheric applications, and its availability is increased recently by extremely fast progress in the tools

for atmospheric and astrophysical studies. For example, the weak lines of the $HD^{18}O$ molecule have been detected in the upper atmosphere of the Earth by the sub-millimeter radiometer instrument aboard the Odin satellite [1]. Recently the lines of this molecule have been identified in the Orion KL hot core spectra recorded by the *Hershel* space observatory [2]. In spite of very low "natural" abundances of the $HD^{18}O$ and $HD^{17}O$ isotopologues (6.23×10^{-7} and 1.16×10^{-7}, respectively), parameters of their spectral lines are included in the current versions of the HITRAN [3] and GEISA [4] spectroscopic databases.

This paper continues our study of the infrared absorption spectra of water vapor enriched by deuterium and oxygen-18. More than 4900 $HD^{18}O$ transitions have been observed between 1090 and 7610 cm^{-1} in Ref. [5]. In addition, more than 3200 $D_2^{18}O$ transitions have been recorded in the 2088–3218 cm^{-1} region [6]. Recently, the analysis of the v_2 bands of both $HD^{18}O$ and $D_2^{18}O$ molecules has been reported in Ref. [7], where about 2500 transitions of the two molecules have been assigned

between 969 and 2148 cm^{-1}. The present paper is devoted to a complete analysis of the high resolution spectrum of a water vapor mixture between 6000 and 9200 cm^{-1}. We were able to assign absorption lines of the $D_2^{18}O$, $HD^{18}O$, $H_2^{18}O$, $D_2^{16}O$, $HD^{16}O$, $H_2^{16}O$ and $H_2^{17}O$ isotopologues. In addition, an unexpected big presence of the deuterated water isotopologues with oxygen-17 (more than 1% of total water concentration) allows us to observe the lines of $D_2^{17}O$ and $HD^{17}O$.

This paper is organized as follows. A brief summary of the experimental conditions and a procedure of the line list preparation are presented in the second section. The trivial vibration–rotation assignments based on the known upper experimental energy levels are outlined in the third section. Section 4 describes the identification of transitions involving new upper energy levels. Section 5 contains a discussion and conclusion.

2. Experimental details and line list preparation

The spectrum was recorded with a Bruker IFS 120 h Fourier transform spectrometer in Hefei, China. Experimental details of the measurements have been presented in our previous papers [5,6]. Here we just give a brief summary of the experimental conditions.

The enriched deuterium and ^{18}O water sample used in the measurements was purchased from ICON services. The spectral region was from 6000 to 9200 cm^{-1}. A Tungsten source, a Ge detector and a CaF$_2$ beam-splitter were used. The unapodized spectral resolution was 0.015 cm^{-1}. A 1.5-m base path length adjustable multi-pass gas cell operated around 297 K was used. The 105-m path length and 1935 Pa sample pressure were adopted for the spectra recording.

A preliminary line list was obtained by the Bruker OPUS spectroscopy software. The complete line list and the line parameters (positions and intensities) were determined using the least squares multi-line fitting program SpectraPlot [8] assuming a Voigt profile. For 2052 isolated lines the Lorenz half-width was fitted in order to improve the quality of the spectra simulation. Previously published line positions of $H_2^{16}O$ [9,10], $H_2^{18}O$ [11], $HD^{16}O$ [12,13] and $D_2^{16}O$ [13] were used for the calibration of measured line positions. The accuracy of the line positions of unblended and not-very-weak lines was estimated to be about 0.0009 cm^{-1}. The overview of the recorded spectrum is given in Fig. 1. Two examples illustrating the quality of spectra near 7714 cm^{-1} (upper panel) and 8622 cm^{-1} (lower panel) with the molecular isotopologue assignments are shown in Fig. 2.

The obtained line intensities of $H_2^{16}O$, $H_2^{18}O$, $HD^{16}O$ and $D_2^{16}O$ were compared with those of Refs. [9,11–13], respectively. This comparison allows us to estimate relative concentrations given in Table 1. The natural abundances of different isotopologues from the HITRAN database [3] are given in the last column of Table 1 for a comparison. The $H_2^{17}O$ abundance was estimated to be about 0.011% against 0.037% of a natural abundance of this species by comparison of observed $H_2^{17}O$ intensities with those of Ref. [3]. In spite of such low ^{17}O enrichment we were able to assign the lines of $HD^{17}O$ and $D_2^{17}O$ molecules in the studied spectrum. This is due to very high HDO/H$_2$O and D$_2$O/HDO ratios. Variational intensities [14] of the $HD^{18}O$, $D_2^{18}O$, $HD^{17}O$ and $D_2^{17}O$ transitions were used for a comparison to the values obtained from the recorded spectrum since no experimental data for these molecules were available in the region under study.

A full line list of 14,170 lines is given as Supplementary Material to this paper. The list includes observed positions of all recorded lines and observed intensities of unsaturated lines followed by the vibration–rotation assignments. Calculated intensity values [14] are also given for
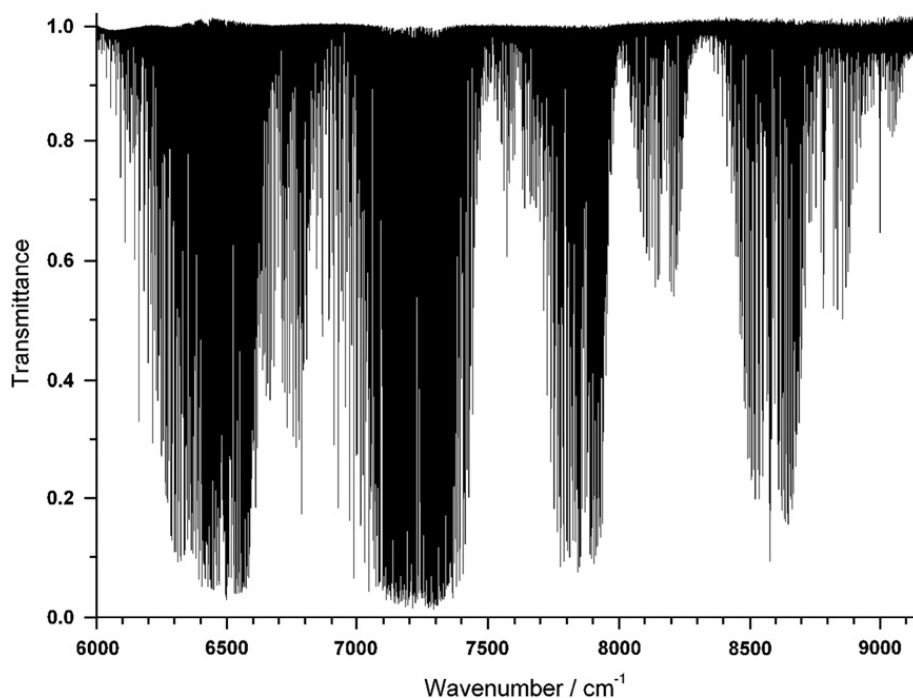
Fig. 1. Overview of the recorded spectrum between 6000 and 9200 cm^{-1}.
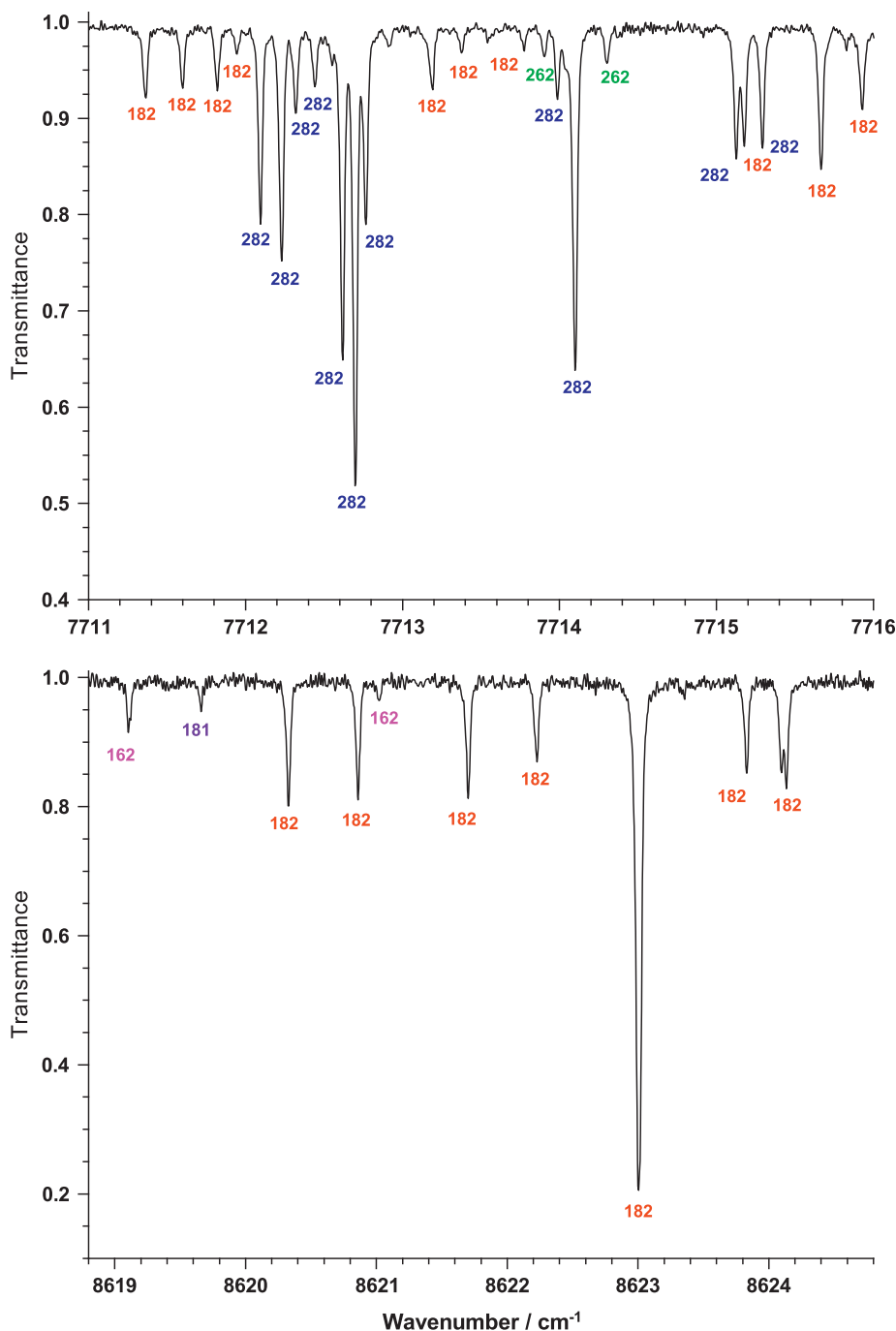
Fig. 2. Two examples illustrating the quality and assignments of the recorded spectrum.

each vibration–rotation transition. The values of all intensities are multiplied by the abundance factors of Table 1.

3. "Trivial" line assignments

The lines of nine water isotopologues were found to contribute in the recorded spectrum. In this section we describe a procedure of the "trivial assignments" of lines for seven isotopic species. The so-called "trivial assignment" is a direct comparison of the obtained linelist with both the previous measured line positions and with the "reference" lists generated from previously reported experimental energy levels completed by calculated line

intensities from Ref. [14].All the $H_2{}^{16}O$, $H_2{}^{18}O$, $H_2{}^{17}O$, $D_2{}^{16}O$ and $HD^{16}O$ lines and some of the $HD^{18}O$ and $D_2{}^{18}O$ lines were assigned using this procedure. General information about the number of assigned lines of different species is given in Table 2.

3.1. $H_2{}^{16}O$, $H_2{}^{18}O$ and $H_2{}^{17}O$

The absorption spectrum of the $H_2{}^{16}O$ molecule in the range 6000–9200 cm^{-1} has been studied by different techniques in numerous papers. The first studies of high resolution spectra in this region have been made using Fourier transform spectroscopy (FTS) [15–19]. Later, a lot

Table 1
Estimated concentrations of different isotopologues in the studied water sample.

Isotopologue	Concentration (%)	
	Estimated	Natural, Ref. [3]
$H_2{}^{17}O$	0.011	0.0371884
$HD^{17}O$	0.169	1.15853×10^{-5}
$D_2{}^{17}O$	0.845	$< 1 \times 10^{-9}$ [a]
$H_2{}^{16}O$	0.098	99.7317101
$HD^{16}O$	1.568	0.0310693
$D_2{}^{16}O$	7.132	2.42×10^{-6a}
$H_2{}^{18}O$	0.946	0.199983
$HD^{18}O$	15.548	6.23003×10^{-5}
$D_2{}^{18}O$	73.683	$< 5 \times 10^{-9}$ [a]

[a] Calculated value from the abundances of hydrogen and oxygen isotopes according to De Biévre P, Gallet M, Holden NE, Barnes IL. Isotopic abundances and atomic weights of the elements. J Phys Chem Ref Data 1984;13:809–92.

Table 2
Summary of the assignments of observed water lines.

Molecule	Number of observed lines		J_{max}	Spectral range (cm^{-1})
	Totally	New		
$H_2{}^{16}O$	450		13	6682–8942
$H_2{}^{18}O$	1111	10	14	6564–9137
$H_2{}^{17}O$	104	3	9	6734–8884
$HD^{16}O$	2015	173	17	6059–8777
$D_2{}^{16}O$	1126	60	16	6056–9123
$HD^{18}O$	4641	2596	19	6000–9183
$D_2{}^{18}O$	3722	3436	19	6001–9109
$HD^{17}O$	589	589	15	6120–8693
$D_2{}^{17}O$	218	218	14	6264–7969
Unassigned	194			6001–9183
Totally	14,170			

of weak lines have been found by long path FTS observations [9,10,20–24]. A number of observations between 6000 and 9200 cm^{-1} have been performed using different types of laser spectrometers [25–30]. The last version of the HITRAN database [3] includes about 6200 transitions of $H_2{}^{16}O$ in the region of interest. We were able to assign 516 transitions of seven vibrational bands in the recorded spectrum. All these lines are included in the HITRAN database. It is found that the positions of 260 isolated and not-very-weak presently observed lines coincide with those of Toth [9] with a root mean square (RMS) deviation of 0.0012 cm^{-1}. Comparison of 42 line positions of isolated lines to data of Tolchenov and Tennyson [10] gives a $RMS = 0.0039$ cm^{-1}.

The spectra of the $H_2{}^{18}O$ molecule between 6000 and 9200 cm^{-1} have been observed mainly by FTS in Refs. [11,31–35] and by the cw-CRDS technique [36]. Numerous additional $H_2{}^{18}O$ lines have been recorded in natural abundance water samples by long path FTS observations [10,23], by high sensitivity cw-CRDS technique [26,27,30] and by a spectrometer with a fiber-coupled distributed feedback diode laser [37]. Overall, more than 6200 transitions have been observed and assigned in previous studies. The last version of the HITRAN database [3] includes 1873 transitions of $H_2{}^{18}O$ between 6000 and 9200 cm^{-1}. We were able to assign 1262 transitions of 11 vibrational bands in the studied spectrum. All these lines, but ten, have been reported in previous studies. More than 700 observed transitions corresponding to not-very-weak ($I^{OBS} > 1 \times 10^{-25}$ cm^{-1}/molecule cm^{-2}) isolated lines were compared with results of Toth [11], Tolchenov and Tennyson [10] and with data included in the HITRAN database [3]. Comparison gives the RMS deviations of 0.0011 and 0.0036 cm^{-1} for Refs. [11] and [10], respectively. Comparison of our data with those of Ref. [3] confirms the conclusion of Liu et al. [35] about the presence in the HITRAN database of inaccurate simulated lines mainly belonging to the $v_1 + v_2 + v_3$, $3v_2 + v_3$ and $v_2 + 2v_3$ bands of the $H_2{}^{18}O$ molecule. The discrepancies between line positions of about 160 transitions of the above mentioned bands observed in the studied spectrum and those of Ref. [3] are between 0.1 and 22 cm^{-1}.

Absorption of the $H_2{}^{17}O$ molecule between 6000 and 9200 cm^{-1} has been studied by FTS in Refs. [11,31,35]. Similar to the $H_2{}^{18}O$ isotopologue numerous $H_2{}^{17}O$ lines have been observed in natural abundance water samples by long path FTS observations [10,23] and by the high sensitivity cw-CRDS technique [26,27,30]. Overall, about 1900 transitions have been observed and assigned in previous studies. The last version of the HITRAN database [3] includes 1235 transitions of $H_2{}^{17}O$ between 6000 and 9200 cm^{-1}. We were able to assign 130 transitions of five vibrational bands in the studied spectrum. All these lines, but three, have been reported in previous studies. Comparison of 73 line positions of isolated lines to data of Toth [11] gives a $RMS = 0.0014$ cm^{-1}. Note, the lines of the $H_2{}^{17}O$ transitions are much weaker than the $H_2{}^{16}O$ and $H_2{}^{18}O$ lines.

All published experimental vibration–rotation transitions of the $H_2{}^{18}O$ and $H_2{}^{17}O$ isotopologues have been recently collected and validated by the International Union of Pure and Applied Chemistry task group (IUPAC TG) [38], where large sets of consistent energy levels have been derived for both considered isotopologues. The accuracy of centers of the presently observed $H_2{}^{18}O$ and $H_2{}^{17}O$ lines was examined by the comparison with those calculated from upper and lower energy levels provided by the IUPAC TG database [38]. The RMS deviations between the full set of our line positions and those calculated from the IUPAC TG energy levels were found to be of 0.0027 and 0.0034 cm^{-1} for $H_2{}^{18}O$ and $H_2{}^{17}O$, respectively. In the case of non-blended and not-very-weak transitions the RMS deviations are 0.0018 and 0.0015 cm^{-1} for the above mentioned species, respectively.

3.2. HD^{16}O and D$_2$^{16}O

Absorption spectra of the $HD^{16}O$ and $D_2{}^{16}O$ isotopologues are less known in the 6000–9200 cm^{-1} spectral region in comparison with those of the $H_2{}^{16}O$ and $H_2^{18}O$ isotopologues.

The spectra of the $HD^{16}O$ molecule between 6000 and 9200 cm^{-1} have been observed by FTS in Refs. [12,39–41] and by laser methods in [42,43] using deuterated water samples. Additional $HD^{16}O$ lines have been obtained in

natural abundance water samples in Refs. [10,23,26, 27,36,44]. Overall, more than 6900 transitions have been observed and assigned in previous studies. The latest version of the HITRAN database [3] includes about 1310 transitions of $HD^{16}O$ between 6000 and 9200 cm^{-1}. In the present study, 2384 transitions of 12 vibrational bands have been attributed to the $HD^{16}O$ molecule. In spite of the low concentrations of $HD^{16}O$ (about 1.6%, see Table 1) and $D_2^{16}O$ (about 7.1%, see Table 1) we were able to assign new transitions of these isotopologues in comparison with previous observations. 173 transitions of eight bands of the $HD^{16}O$ molecule were observed for the first time. A major part of the newly observed transitions belongs to the $5v_2$, $2v_3$ and v_2+2v_3 bands. The root mean square deviation between all observed transitions and line positions calculated from the IUPAC TG energy levels [45] was estimated to be of 0.0027 cm^{-1}. A set of about 1600 selected transitions agrees with IUPAC TG results with a $RMS=0.0015$ cm^{-1}. The RMS deviation between our line positions and those of Ref. [13] was found to be around 0.0015 cm^{-1}.

Recordings of high resolution $D_2^{16}O$ absorption spectra in the region of interest started from the studies of Dickey et al. [46] and Benedict et al. [47]. Later studies on $D_2^{16}O$ have been performed by FTS setup [48–53] and by DFB semiconductor laser spectroscopy [42,44]. An extended analysis of the $D_2^{16}O$ absorption spectrum between 8800 and 9520 cm^{-1} has been done by using combination of FTS and ICLAS-VeCSEL technique [54]. Overall, more than 5219 transitions have been observed and assigned in previous studies in the 6000–9200 cm^{-1} region. We were able to assign 1438 transitions of 14 vibrational bands in the studied spectrum. 60 transitions of 11 bands were observed for the first time. Note some experimental energy levels used for the assignment of the $D_2^{16}O$ lines originate from the studies of emission spectra in the 380–1880 cm^{-1} [55] and 2077–4323 cm^{-1} [56] spectral ranges. Obtained line intensities were used for determination of the $D_2^{16}O$ concentration by comparison with experimental [13] and with variational [14] intensities. Positions of all presently observed $D_2^{16}O$ transitions agree with Refs. [48,53,54] data with a RMS deviation of 0.0029 cm^{-1}. For the 1077 selected transitions this discrepancy is on the order of 0.0016 cm^{-1}.

3.3. $HD^{18}O$

Critical evaluation of the experimental studies of high resolution vibration–rotation spectra of $HD^{18}O$ has been done in Ref. [57] and later in Ref. [45]. There is only one study focused especially on the $HD^{18}O$ spectrum: Liu et al. [5] reported about 5000 transitions from 1090 to 7610 cm^{-1}. Only 525 transitions of the $2v_3$ band between 6657 and 7610 cm^{-1} of Ref. [5] intersect with our spectral region. Mikhailenko et al. [57,58] found about 1100 transitions of $HD^{18}O$ among $HD^{16}O$ and $D_2^{16}O$ lines coming from long-path Fourier transform spectra of deuterated water recorded by the Reims-Brussels group [13] in the 6000–9130 cm^{-1} spectral range. The lines of six new bands ($2v_3$, v_2+2v_3, $v_1+v_2+v_3$, $2v_1+v_3$, $3v_2+v_3$, and $3v_1$) with respect to those of Ref. [5] have been reported in Refs. [57,58].

Furthermore, 1099 $HD^{18}O$ transitions have been found by Liu et al. [36] in high sensitivity CW-CRDS spectrum of ^{18}O-enriched water vapor between 6000 and 6722 cm^{-1}. Overall, more than 2050 transitions of 11 bands have been observed in Refs. [5,36,57,58].

The most complete list of 1860 rotational energies of 29 vibrational states of $HD^{18}O$ has been published in the IUPAC TG review [45]. These energies have been determined from 8634 transitions between 0.2 and 12,105 cm^{-1}. Comparison of the "reference" list generated using energy levels from [45] and variational intensities [14] allowed for trivial assignment of 3795 transitions with a RMS deviation for line positions being on the order of 0.003 cm^{-1}.

3.4. $D_2^{18}O$

A review of the experimental studies of high resolution vibration–rotation spectra of $D_2^{18}O$ has been done in Ref. [58]. Rotational, fundamental and $2v_2$ bands have been analyzed in Refs. [6,59–64]. Note that Toth [65] reported experimental energy levels for the (011) vibration state but no corresponding transitions for the v_2+v_3 band. Extended analysis of the v_2 band of $D_2^{18}O$ has recently been reported in Ref. [7] where more than 1150 transitions have been assigned between 969 and 1606 cm^{-1}. No spectral data above 3200 cm^{-1} exist in the literature except 286 transitions [58] of seven bands ($3v_2+v_3$, $v_1+v_2+v_3$, $2v_1+v_2$, $v_1+2v_2+v_3$, $2v_1+v_3$, $3v_1$, and $3v_3$) between 6127 and 8246 cm^{-1}. 433 $D_2^{18}O$ lines could be trivially assigned based on experimental lower and upper energy levels [7,58] and variational intensities [14]. Line positions were found to agree within 0.0023 cm^{-1}.

3.5. $HD^{17}O$ and $D_2^{17}O$

$HD^{17}O$ and $D_2^{17}O$ obviously are among the least investigated water isotopologues. Thus, $HD^{17}O$ experimental studies are limited by observations of 61 hyperfine components of 21 pure rotational transitions in the ground vibrational state between 8817 and 241 636.5 MHz [66,67], and 433 transitions between 1118 and 1674 cm^{-1} belonging to the v_2 band [68]. Note, the hyperfine structure of the $2_{2\,0} \rightarrow 2_{1\,1}$ pure rotational transition of $HD^{17}O$ at 10 374 MHz has been also investigated by Verkhoeven et al. [69]. For the $D_2^{17}O$ isotopologue, 63 hyperfine components of 19 microwave transitions between 21,311 and 399,652 MHz in the ground vibrational state are reported in Ref. [59] and 226 transitions of the v_2 band between 995 and 1390 cm^{-1} are assigned in Ref. [70]. No experimental vibration–rotation transitions are reported for the $HD^{17}O$ and $D_2^{17}O$ isotopologues above 1680 cm^{-1}.

4. Assignment of new $HD^{18}O$, $D_2^{18}O$, $HD^{17}O$ and $D_2^{17}O$ absorption lines and energy level determination

About 7000 absorption lines left unassigned after a comparison with the known experimental data in Section 3 have been further treated using high-accuracy variational calculations. The calculated spectra taken from the web site of the SPECTRA system [14] have been used for the line assignments of $HD^{18}O$, $D_2^{18}O$, $HD^{17}O$ and $D_2^{17}O$.

These data are the results of variational calculations made by S.A. Tashkun (Tomsk, Russia) using the VTET computer code of Schwenke [71,72] and the potential energy and dipole moment surfaces of Partridge and Schwenke [73,74]. Hereafter, these data will be referred to as PS calculated line positions and line intensities. General information about the number of assigned lines of different species is given in Table 3.

In the spectrum assignments we relied on the known smooth $(E^{OBS}-E^{PS})$ variations for the rovibrational levels having the same rotational number K_a and vibrational quantum numbers $(V_1V_2V_3)$ with increase of rotational quantum number J. Examples of such variations for the $D_2\,{}^{18}O$ molecule in case of $K_a=0$ are shown in Fig. 3; they were used for evaluation of the E_{VIB} terms for some of the vibrational states in case if the corresponding experimental transitions involving the $J_{KaKc}=0_{0\ 0}$ upper level were not observed. The $(E^{OBS}-E^{PS})$ deviations can change significantly depending on the vibrational state (from

-0.18 cm^{-1} for the (0 0 3) state up to $+0.15$ cm^{-1} for the (3 0 0) state in Fig. 3), and can be distorted due to close resonances (as is seen for the (0 0 3) vibrational state for $J=10$).

Matching between the observed (I^{OBS}) and calculated (I^{PS}) line intensities represented the second very important criterion of the assignments. The (I^{OBS}/I^{PS}) ratios for all considered isotopic species are shown in Fig. 4. The comparison was limited to unsaturated and adequately isolated lines. It is obvious from the figure that the experimental intensities agree very well with PS values. Though our experimental intensities have been scaled against PS values, this scaling required just several tens of lines, and a good (I^{OBS}/I^{PS}) intensity matching of the observed and calculated intensity for the retained thousands of lines confirms the good quality of both experimental and variational data. The accuracy of the experimental intensities for the unsaturated, isolated and not-very-weak lines was estimated to be about 10–15%.

Table 3
Statistics on the $HD^{18}O$, $D_2\,{}^{18}O$, $HD^{17}O$ and $D_2\,{}^{17}O$ assigned transitions.

| Band	$D_2\,{}^{18}O$			$HD^{18}O$		
	Num. tra.	J_{min}–J_{max}	Spectral range (cm^{-1})	Num. tra.	J_{min}–J_{max}	Spectral range (cm^{-1})
v_1+v_3				934	0–16	6000–6745
$5v_2$				201	0–14	6093–6901
$3v_2+v_3-v_2$				37	1–8	6226–6427
$v_1+v_2+v_3-v_2$				14	1–8	6289–6475
$2v_2+v_3$				202	0–16	6459–6970
v_1+3v_2	226	0–15	6002–6652	120	0–11	6512–7010
$2v_3$				1536	0–19	6701–7638
$v_2+2v_3-v_2$				129	0–11	7006–7372
$3v_2+v_3$	420	0–15	6002–6653	143	0–11	7559–8007
$4v_2+v_3-v_2$	6	3–7	6156–6217			
$v_1+v_2+v_3$	791	0–19	6157–6908	119	0–11	7579–8754
$2v_1+v_2$	397	0–18	6192–6731	668	0–15	6416–7067
$6v_2$				2	0, 1	7863–7895
v_2+2v_3	416	0–17	6271–6866	610	0–15	8303–8912
$v_1+2v_2+v_3-v_2$	139	0–13	6330–6587			
$2v_1+2v_2-v_2$	9	4–8	6343–6565			
$2v_2+2v_3-v_2$	1	4	6461.583			
$v_1+2v_2+v_3$	335	0–16	7429–7960	4	2–4	9043–9159
$2v_1+2v_2$	81	2–15	7447–7961			
$3v_1$	396	1–15	7507–8265	362	0–13	7631–8099
$2v_2+2v_3$	22	4–9	7564–7952			
$4v_2+v_3$				1	4	8919.337
$2v_1+v_3$	608	0–19	7564–8089	45	1–7	8772–9182
v_1+2v_3	144	1–13	7652–8269			
$2v_1+v_2+v_3-v_2$	24	1–8	7736–7904			
$3v_3$	349	0–16	7936–8324			
$2v_1+v_2+v_3$	168	0–12	8846–9109			
$3v_1+v_2$	4	3–5	8914–9060			
$v_1+v_2+2v_3$	1	5	9080.354			
	$D_2\,{}^{17}O$			$HD^{17}O$		
v_1+v_3				166	1–10	6120–6645
$2v_2+v_3$				55	1–9	6333–6587
$3v_2+v_3$	2	2, 5	6235–6265			
$v_1+v_2+v_3$	183	0–14	6379–6646			
$2v_1+v_2$	16	4–9	6404–6588	68	0–10	6623–6846
$2v_3$				407	0–14	6855–7452
v_2+2v_3				48	0–10	8469–8729
$2v_1+v_3$	78	1–12	7745–7969			
$3v_1$	2	4, 5	7824–7925			
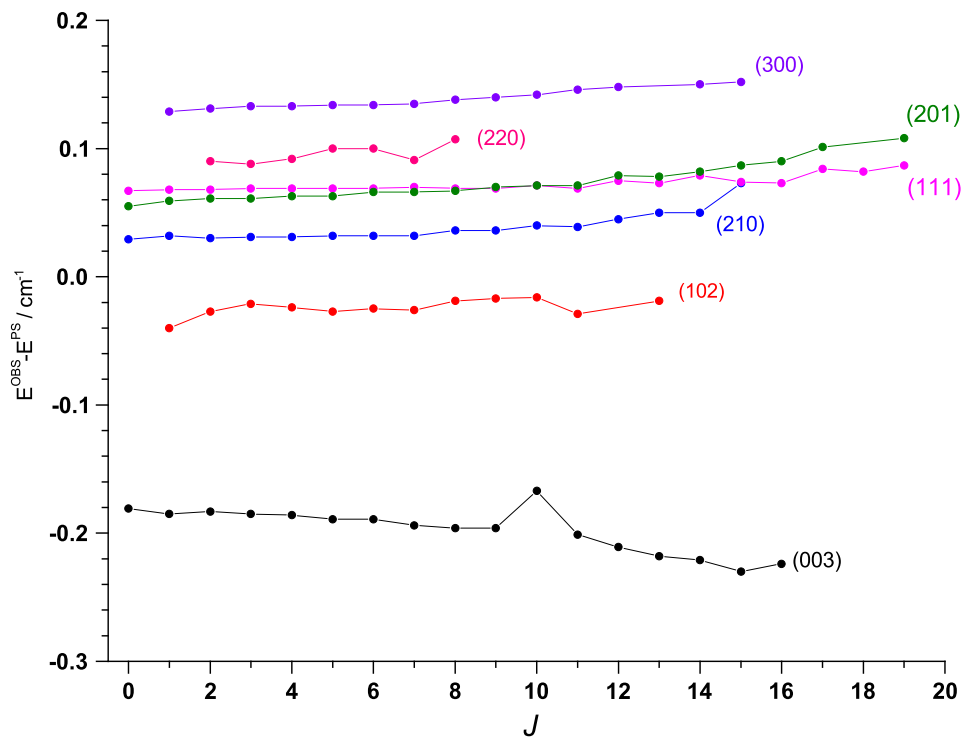
Fig. 3. ($E^{OBS}-E^{PS}$) discrepancies for the energy levels with $K_a=0$ as a function of the rotational J quantum number for some vibrational states of the D_2 ^{18}O molecule.
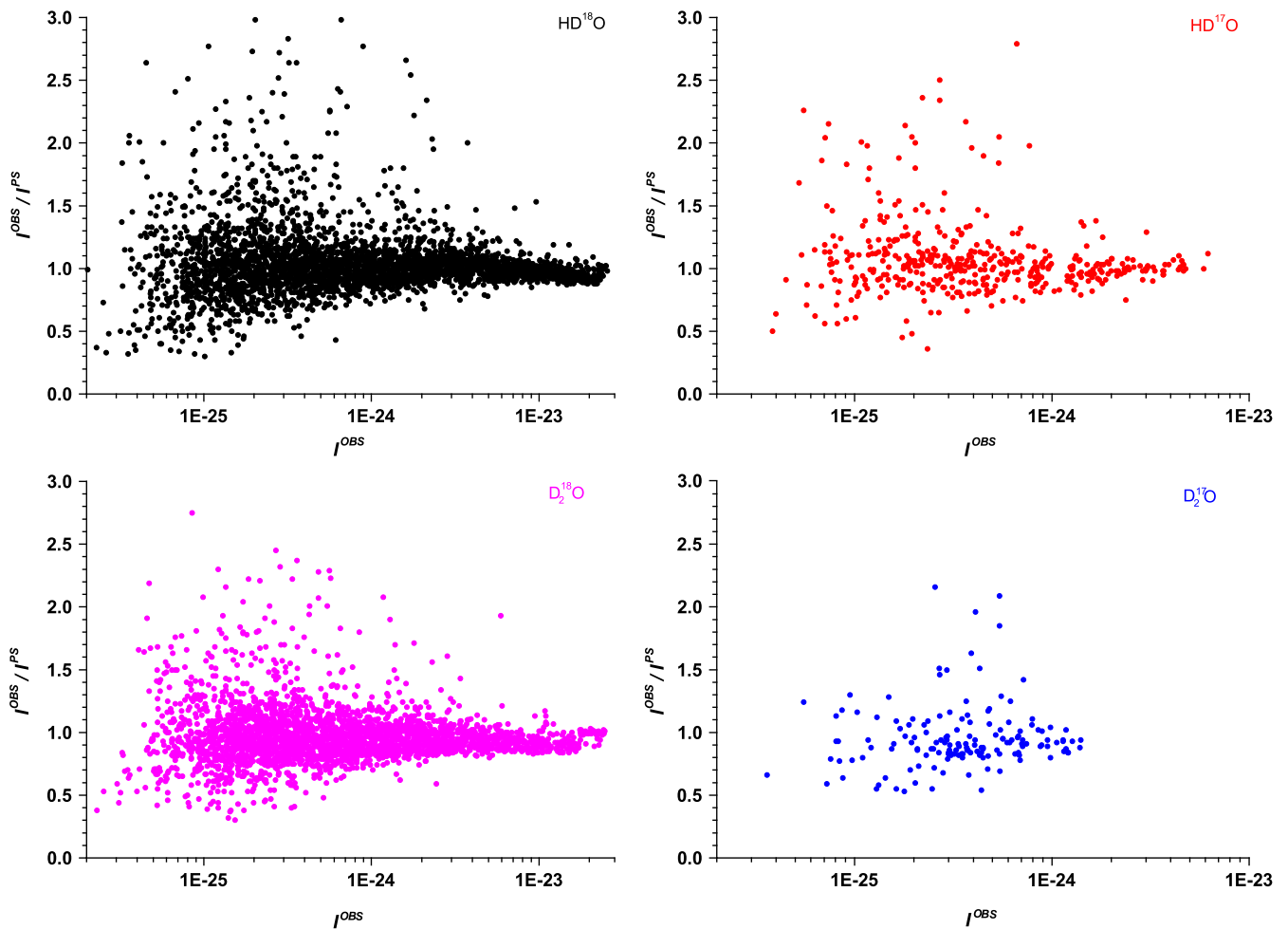

Fig. 4. Ratios of the experimental line intensities (I^{OBS}) by the PS calculated values (I^{PS}) for the HD^{18}O, D$_2$ ^{18}O, HD^{17}O, D$_2$ ^{17}O isotopologues.

The assignments were then automatically attached to the observed line if the calculated intensity was no less than 10% with respect to experimental value. However, the derived experimental intensities of weak and blended lines can be greatly distorted up to 100%.

A complete list of the observed lines is given in Supplementary Material I. It contains 14,170 absorption lines which correspond to more than 16,800 transitions belonging to nine water isotopologues. Only 194 relatively weak lines were left unassigned. The calculated intensity is given for all assigned lines, and the experimental intensity is also attached for the majority of the observed lines.

In the case of saturated or greatly blended lines, the experimental intensity is not included because of the apparent distortion.

Final checking of the consistency of the line assignments as well as experimental energy levels determinations of all four isotopologues were performed by using the RITZ code [57]. This software has been previously successfully applied to determine energy levels for HD^{18}O and D$_2$ ^{18}O [7,57,58] and other water isotopologues [26,27,30,75–77]. The summary of the information on the energy levels retrieved from the spectrum analysis is presented in Table 4.

Table 4
Summary of the HD^{18}O, D$_2$ ^{18}O, HD^{17}O and D$_2$ ^{17}O experimental energy levels derived from the analysis of the recorded spectrum.

Upper vibrational energy (cm^{-1})		Molecule	Upper state, (V$_1$V$_2$V$_3$)	This study			Previously reported
Observed	Calculated, PS			Number of levels	J_{max}	$K_{a\ max}$	Number of levels
6390.9836	6390.98	182	(101)	171	16	10	135
6425.9510	6425.93	182	(021)	151	16	8	109
6659.4513	6659.45	182	(050)	65	14	3	11
6711.6726	6711.60	182	(210)	148	15	8	78
6809.8895	6809.89	182	(130)	43	11	8	
7229.1851	7229.28	182	(002)	215	19	10	133
7724.8251	7724.81	182	(031)	75	11	6	10
7774.7138	7774.71	182	(111)	54	11	8	11
7876.1715	7876.02	182	(300)	112	13	7	46
7878.5988	7878.62	182	(060)	2	1	0	
8583.0842	8583.18	182	(012)	141	15	8	79
	8994.25	182	(041)	1	4	0	
9008.07*	9008.02	182	(201)	29	7	5	2
	9114.59	182	(121)	4	4	2	
In total				1212			614
6084.9214	6084.87	282	(130)	105	15	10	
6191.3530	6191.23	282	(031)	168	15	8	1
6423.0183	6422.99	282	(210)	159	18	8	4
6494.7399	6494.67	282	(111)	234	19	11	43
6640.2591	6640.16	282	(012)	152	17	8	
	7292.79	282	(041)	6	7	5	
7555.70*	7555.60	282	(220)	46	15	6	
7626.7848	7626.68	282	(121)	148	16	10	7
	7771.82	282	(022)	13	9	6	
7819.29*	7819.15	282	(300)	133	15	8	2
7859.1030	7859.05	282	(201)	200	19	10	34
8007.44*	8007.46	282	(102)	78	13	8	
8163.8054	8163.99	282	(003)	144	16	9	6
	8963.44	282	(310)	2	5	3	
9001.4538	9001.40	282	(211)	83	12	7	
	9148.15	282	(112)	1	5	1	
In total				1672			97
6402.5016	6402.67	172	(101)	68	10	7	
6438.16*	6438.40	172	(021)	40	9	5	
6728.2591	6728.55	172	(210)	43	10	5	
7239.2024	7239.50	172	(002)	112	14	7	
8596.2594	8596.62	172	(012)	33	10	4	
In total				296			
	6212.30	272	(031)	1	4	2	
	6437.39	272	(210)	9	7	4	
6512.8589	6513.18	272	(111)	95	12	7	
	7835.33	272	(300)	2	5	3	
7878.25*	7878.61	272	(201)	51	12	5	
In total				158			

Vibrational energies marked by asterisk were estimated from the $E^{OBS} - E^{PS}$ tendency for the energy levels with $K_a = 0$ with accuracy of about ± 0.05 cm^{-1}.

4.1. HD^{18}O

In total, 1212 energy levels belonging to 14 vibrational states were determined for the HD^{18}O isotopologues (see Table 4 for details). They agree well with variational prediction [14] with maximal discrepancy of 0.218 cm^{-1},

and an *RMS* deviation of 0.086 cm^{-1}. Comparison of the energy levels [45] with our data yielded 598 new energy levels. The root mean square deviation between our and IUPAC TG data is 0.002 cm^{-1}.

The new information includes additional energy levels for the previously investigated (002), (012), (210), (300)
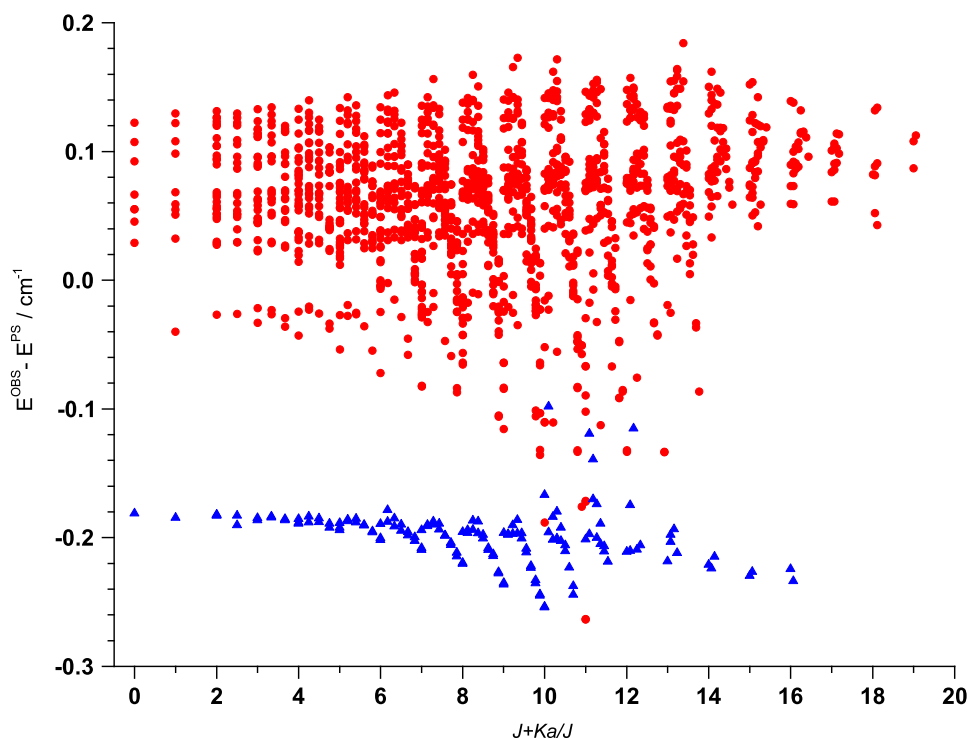
Fig. 5. ($E^{OBS} - E^{PS}$) discrepancies for the total set of derived D$_2$ ^{18}O energy levels. The largest in absolute value deviations involving the (003) energy levels are highlighted (in blue, triangles). (For interpretation of the references to color in this figure, the reader is referred to the web version of this article.)
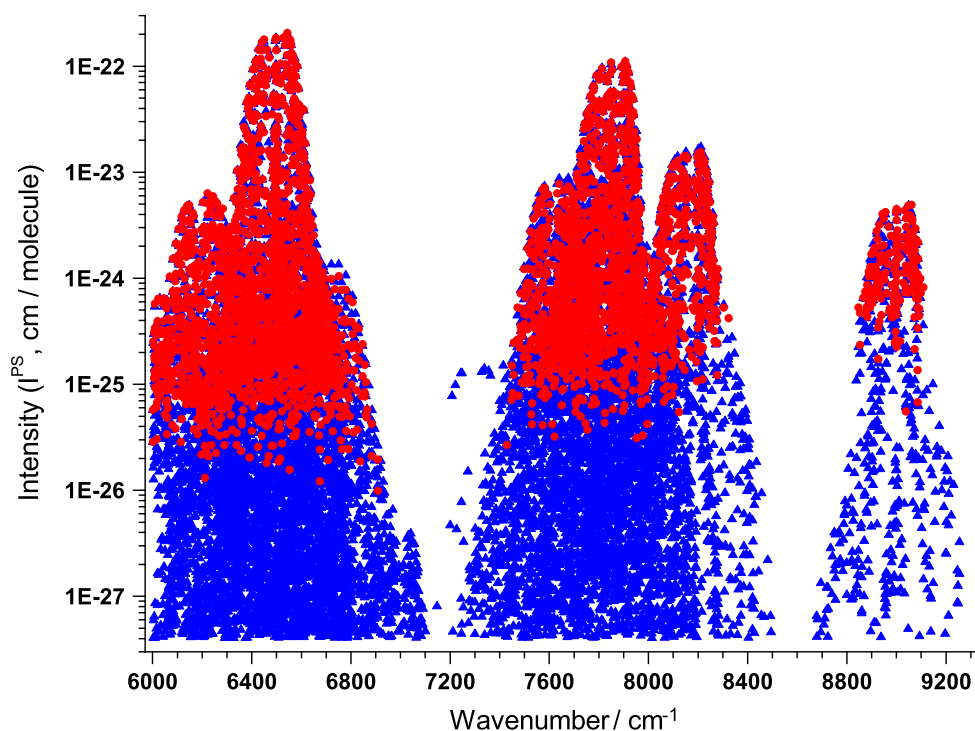
Fig. 6. Comparison of the directly observed absorption lines (in red, circles) to those calculated from the experimental energy levels (in blue, triangles) for the D$_2$ ^{18}O molecule. (For interpretation of the references to color in this figure, the reader is referred to the web version of this article.)

vibrational states (number of energy levels increased by 61%, 78%, 90%, and 140%, respectively). The rotational structure of two new vibrational states (130) and (201) was investigated for the first time. The number of energy levels for the (031), (050), and (111) states was increased by 4 or more times. In total, 6 new vibrational energies have been determined: (050) at 6659.4513, (130) at 6809.8895, (031) at 7274.8251, (111) at 7774.7138, (060) at 7878.5988, and (0 1 2) at 8583.0842 cm^{-1}.

Similar to the HD^{16}O isotopologue (see, for example, Ref. [78]), HD^{18}O also undergoes a strong centrifugal distortion effect which leads to strengthening the high-order resonances and, consequently, to observation of vibration–rotation transitions involving the highly excited bending vibrational states. Thus, we could assign 201 transitions of a very weak $5\nu_2$ band which, similar to HD^{16}O, borrows its intensity through a high-order resonance interaction from the much stronger $2\nu_1+\nu_2$ band. As a result, the observed integrated intensity of the $5\nu_2$ band (3.18×10^{-3} cm^{-1}/(molecule cm^{-2}) at 296 K) is sufficiently larger than that of the $\nu_1+3\nu_2$ band (6.73×10^{-4} cm^{-1}/(molecule cm^{-2}) at 296 K). Note, in the H$_2$^{16}O molecule the situation is quite opposite and only a few weak lines of the $5\nu_2$ band are observed in the absorption spectrum recorded at room temperature. Two assigned transitions of the highly excited $6\nu_2$ band
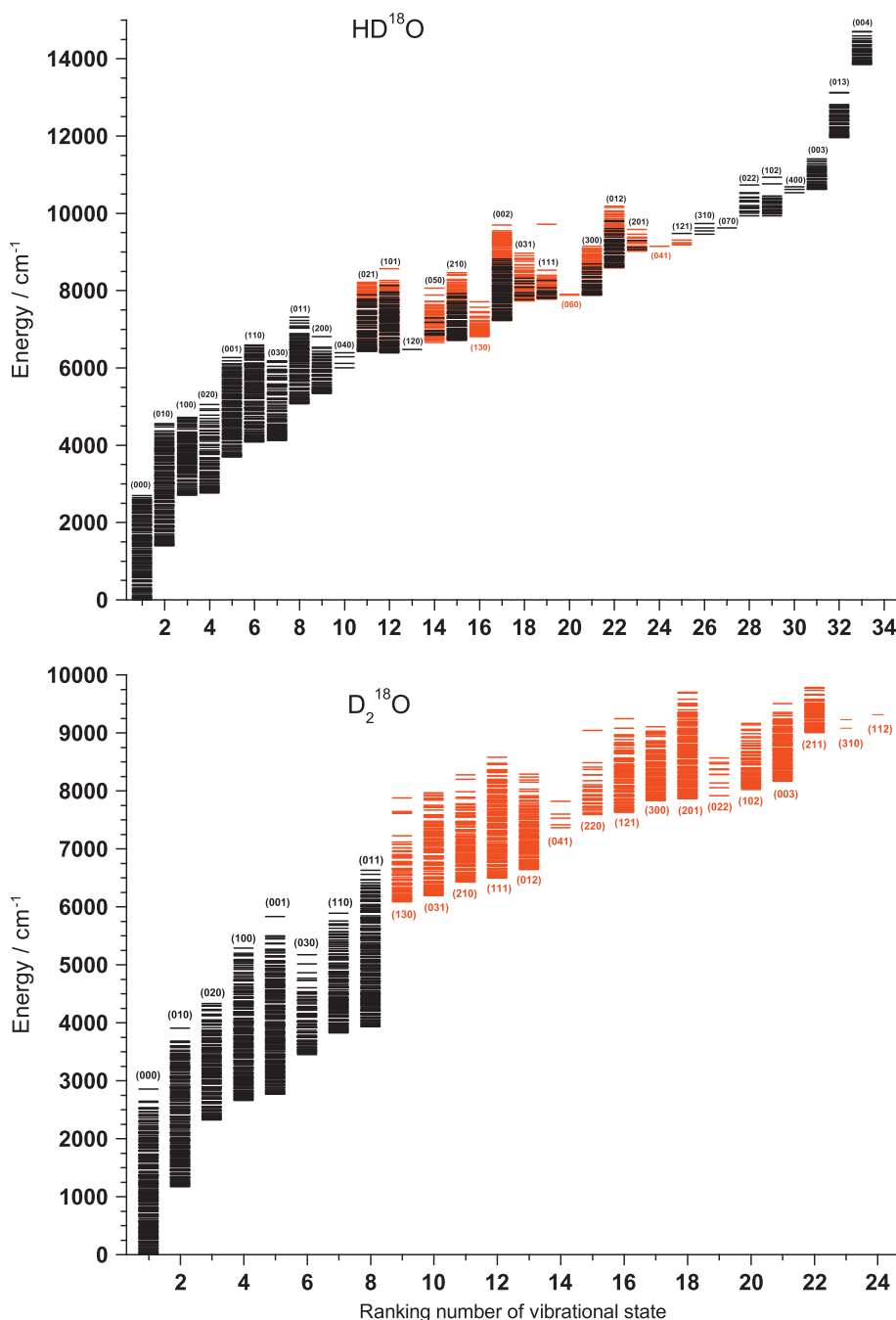
Fig. 7. Overview of the experimental energy levels for the HD^{18}O (upper panel) and D$_2$^{18}O (lower panel) isotopologues.

are also strengthened by the resonance interaction with the $3\nu_1$ band.

4.2. $D_2{}^{18}O$

Good matching between experimental (ν^{OBS}) and variational (ν^{PS}) line positions and intensities is also found in case of $D_2{}^{18}O$. The root mean square and maximal deviations between the experimental and PS energy levels were

found to be about 0.098 and 0.264 cm^{-1}, respectively. Fig. 5 shows the ($E^{OBS} - E^{PS}$) deviations for the total set of derived $D_2{}^{18}O$ energy levels, the largest deviations in absolute value involving the (003) energy levels are highlighted. A large number of 1665 energy levels belonging to 16 vibrational states (see Table 4) was obtained for the $D_2{}^{18}O$ isotopologue, while only 101 energy levels, mostly for the (111) and (201) states, were previously known [58]. Our energy levels in common agree well with the values of Ref. [58] with a *RMS* deviation of 0.003 cm^{-1}. An accurate and

Fig. 8. ($E^{OBS} - E^{PS}$) discrepancies for the total set of derived HD^{17}O (in circles, upper panel) and D$_2{}^{17}$O (in triangles, lower panel) energy levels.

Table 5
New experimental energy levels of the $HD^{17}O$ molecule.

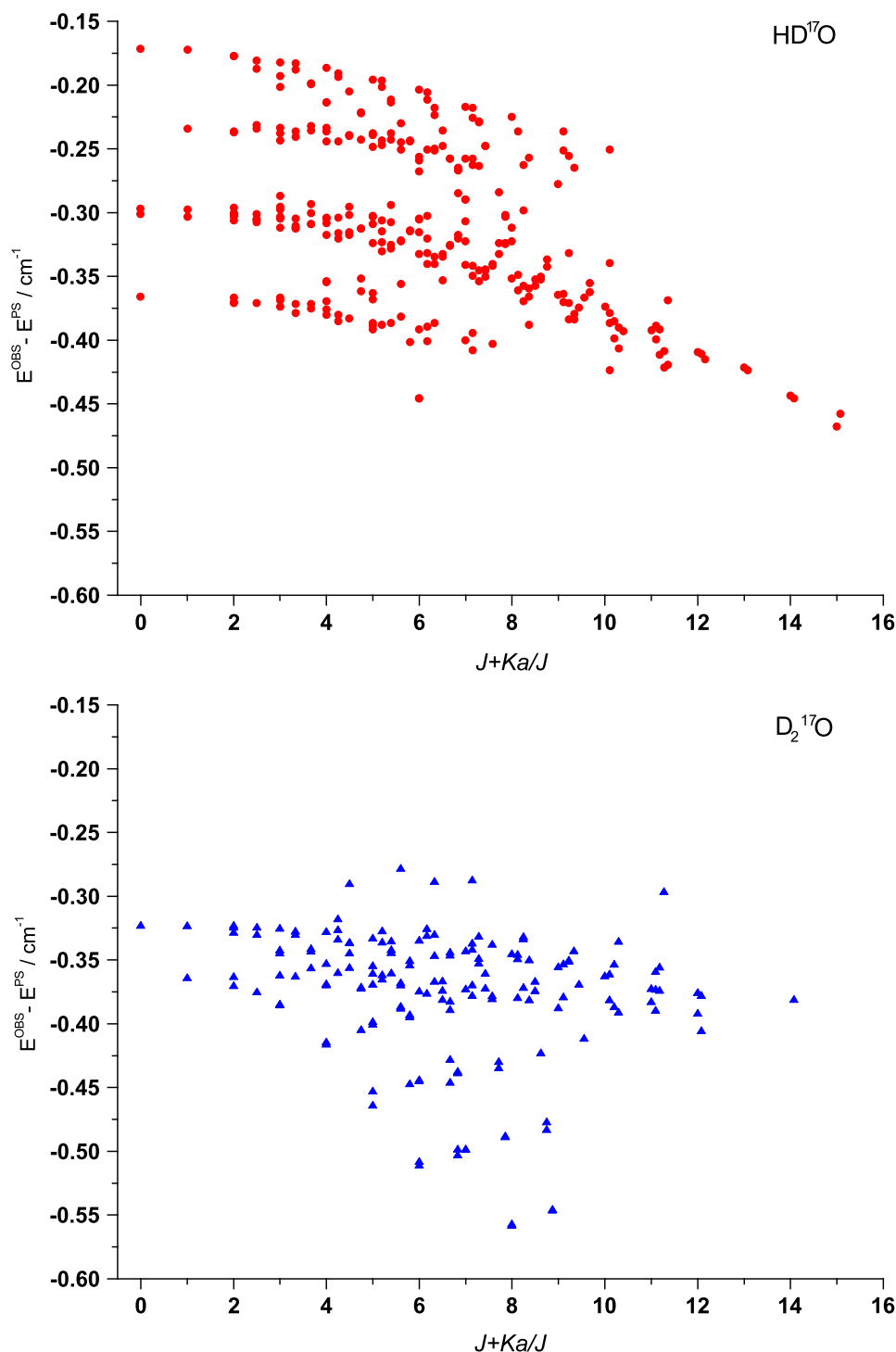| Vib	J	K_a	K_c	E^{OBS}	dE	Nt
002	0	0	0	7239.2024	0.6	2
002	1	0	1	7254.4860	0.6	4
002	1	1	1	7266.6368	0.3	2
002	1	1	0	7269.4624	0.3	4
002	2	0	2	7284.6088	0.5	3
002	2	1	2	7294.3702	0.3	7
002	2	1	1	7302.8383	0.4	3
002	2	2	1	7339.1657	0.3	4
002	2	2	0	7339.6005	0.4	3
002	3	0	3	7328.7472	0.3	5
002	3	1	3	7335.7046	0.3	4
002	3	1	2	7352.5787	0.3	5
002	3	2	2	7384.9601	0.2	6
002	3	2	1	7387.0715	0.4	3
002	3	3	1	7452.3973	0.5	3
002	3	3	0	7452.4389	0.3	5
002	4	0	4	7385.9639	0.3	5
002	4	1	4	7390.3771	0.3	5
002	4	1	3	7418.2379	0.2	5
002	4	2	3	7445.6480	0.3	4
002	4	2	2	7451.5820	0.2	6
002	4	3	2	7514.1246	0.2	4
002	4	3	1	7514.4172	0.3	5
002	4	4	1	7606.6863	0.6	4
002	4	4	0	7606.6858	0.8	2
002	5	0	5	7455.5809	0.2	4
002	5	1	5	7458.1202	0.3	4
002	5	1	4	7499.1376	0.4	4
002	5	2	4	7520.9181	0.2	6
002	5	2	3	7533.4475	0.2	7
002	5	3	3	7591.3846	0.3	5
002	5	3	2	7592.5191	0.3	4
002	5	4	2	7683.7156	0.4	5
002	5	4	1	7683.7464	0.6	2
002	5	5	1	7801.3546	0.8	3
002	5	5	0	7801.3544	0.8	3
002	6	0	6	7537.3349	0.4	5
002	6	1	6	7538.6939	0.4	2
002	6	1	5	7594.3545	0.4	3
002	6	2	5	7610.4134	0.3	5
002	6	2	4	7632.4530	0.2	7
002	6	3	4	7684.0845	0.3	5
002	6	3	3	7687.3053	0.2	4
002	6	4	3	7776.3528	0.6	3
002	6	4	2	7776.5005	0.4	4
002	6	5	2	7893.5082	1.6	2
002	6	5	1	7893.5079	1.4	2
002	6	6	1	8035.4505	1.4	2
002	6	6	0	8035.4509	1.5	2
002	7	0	7	7631.2244	0.6	3
002	7	1	7	7631.9173	0.6	4
002	7	1	6	7702.8359	0.7	2
002	7	2	6	7713.7372	0.5	4
002	7	2	5	7747.9880	0.6	2
002	7	3	5	7792.0234	0.4	3
002	7	3	4	7799.3964	0.3	3
002	7	4	4	7884.6428	0.5	2
002	7	4	3	7885.1705	0.4	3
002	7	5	3	8001.1751	0.5	2
002	7	5	2	8001.1900	2.2	2
002	7	6	2	8142.5884	1.0	2
002	7	6	1	8142.5879	1.1	2
002	7	7	1	8307.9036	2.9	1
002	7	7	0	8307.9037	2.7	1
002	8	0	8	7737.3119	0.6	2
002	8	1	8	7737.6557	0.7	3
002	8	1	7	7823.6708	0.7	2
002	8	2	7	7830.5037	0.6	3
002	8	2	6	7879.1955	0.8	2
002	8	3	6	7914.8936	0.3	2
002	8	3	5	7929.1947	0.5	4
002	8	4	5	8008.5883	0.3	2
002	8	4	4	8010.0971	1.0	1
002	8	5	4	8124.4304	0.6	2
002	8	5	3	8124.4955	0.8	2
002	8	6	3	8265.1469	1.7	2
002	8	6	2	8265.1431	1.8	2
002	9	0	9	7855.6454	0.7	4
002	9	1	9	7855.8099	0.7	4
002	9	1	8	7956.3557	1.1	1
002	9	2	8	7960.3536	0.8	3
002	9	2	7	8025.0270	0.8	3
002	9	3	7	8052.3061	1.0	1
002	9	3	6	8076.6059	0.7	3
002	9	4	5	8151.7659	1.0	1
002	9	5	5	8263.3159	1.3	1
002	9	6	4	8403.1506	2.2	2
002	9	6	3	8403.1524	3.1	1
002	10	0	10	7986.2492	0.9	2
002	10	1	10	7986.3229	1.2	2
002	10	1	9	8100.7694	1.4	1
002	10	2	9	8102.9918	1.1	1
002	10	2	8	8184.3193	0.9	2
002	10	3	8	8203.8325	1.6	1
002	10	3	7	8241.0311	1.6	2
002	10	4	7	8302.9866	1.0	1
002	11	0	11	8129.1148	1.5	2
002	11	1	11	8129.1500	1.3	3
002	11	1	10	8257.0009	1.6	1
002	11	2	10	8258.1958	3.9	1
002	11	2	9	8355.9855	1.5	1
002	11	3	9	8369.0087	1.2	1
002	11	3	8	8421.5464	2.2	1
002	11	4	8	8472.9455	1.0	1
002	11	4	7	8487.5148	1.0	1
002	12	0	12	8284.2214	3.7	1
002	12	1	12	8284.2362	1.9	1
002	12	2	11	8425.7743	1.3	1
002	13	0	13	8451.5521	1.9	1
002	13	1	13	8451.5572	1.9	1
002	14	0	14	8631.0657	3.2	2
002	14	1	14	8631.0659	3.2	2
012	0	0	0	8596.2594	1.1	1
012	1	1	1	8625.3302	1.0	1
012	1	1	0	8628.3856	0.2	2
012	2	0	2	8641.8380	0.7	2
012	2	1	1	8662.1139	0.3	2
012	2	2	1	8703.0775	1.0	1
012	2	2	0	8703.5298	0.2	2
012	3	0	3	8686.0982	1.0	1
012	3	1	3	8694.1456	1.0	1
012	3	1	2	8712.3664	0.6	2
012	3	2	2	8749.0593	1.0	1
012	3	2	1	8751.2556	1.0	1
012	3	3	1	8824.4953	1.0	1
012	3	3	0	8824.5433	1.0	1
012	4	0	4	8743.3844	1.0	1
012	4	1	4	8748.5841	0.4	2
012	4	1	3	8778.6891	0.5	2
012	4	2	3	8809.9847	1.0	1
012	4	3	1	8886.8203	0.5	2
012	4	4	1	8989.6828	1.2	1
012	4	4	0	8989.6817	1.2	1
012	5	0	5	8812.9570	1.0	1
012	5	1	4	8860.3793	1.0	1
012	5	2	4	8885.5394	1.0	1
012	5	3	2	8965.2707	1.0	1
012	6	0	6	8894.4952	1.0	1

Table 5 (continued)

Table 5 (*continued*)

Vib	J	K_a	K_c	E^{OBS}	dE	Nt
012	6	1	6	8896.1720	1.0	1
012	6	1	5	8956.4879	1.0	1
012	6	2	5	8975.3446	1.0	1
012	7	0	7	8987.9837	0.5	2
012	7	1	7	8988.8634	1.0	1
012	7	1	6	9065.9126	1.1	1
012	10	1	10	9340.8774	1.2	1
021	1	0	1	6453.6019	1.0	1
021	1	1	0	6473.2624	0.2	2
021	2	0	2	6484.0684	1.0	1
021	2	1	2	6497.9358	1.0	1
021	2	1	1	6507.2069	0.3	2
021	2	2	1	6557.1561	1.0	1
021	2	2	0	6557.5490	1.0	1
021	3	0	3	6528.8038	1.0	1
021	3	1	3	6539.3391	0.2	2
021	3	1	2	6557.9683	1.0	1
021	3	2	2	6603.4999	1.0	1
021	3	2	1	6605.4340	1.0	1
021	3	3	1	6694.3714	1.0	1
021	3	3	0	6694.3993	0.7	2
021	4	0	4	6586.8774	1.0	1
021	4	1	4	6594.1416	1.0	1
021	4	2	3	6664.9429	1.0	1
021	4	2	2	6670.4847	0.2	2
021	4	3	2	6756.8122	0.6	2
021	5	0	5	6657.4740	0.5	2
021	5	1	5	6662.0739	1.0	1
021	5	1	4	6707.7868	0.8	2
021	5	2	4	6741.2181	1.0	1
021	5	2	3	6753.1891	0.2	2
021	5	3	3	6834.9771	1.0	1
021	5	3	2	6835.8433	0.2	2
021	5	5	1	7115.5997	1.2	1
021	5	5	0	7115.5998	1.1	1
021	6	0	6	6740.1535	1.0	1
021	6	1	5	6805.5098	1.0	1
021	6	2	5	6831.9769	1.0	1
021	6	2	4	6853.3785	1.0	1
021	6	5	2	7208.8192	1.3	1
021	6	5	1	7208.8182	1.5	1
021	7	0	7	6834.8114	1.0	1
021	7	1	7	6836.3376	1.0	1
021	7	1	6	6917.1742	1.0	1
021	7	2	6	6936.8465	1.0	1
021	8	2	6	7105.4018	1.0	1
021	9	0	9	7060.1968	0.8	2
101	0	0	0	6402.5016	1.0	1
101	1	0	1	6417.6500	0.2	2
101	1	1	1	6431.4131	0.5	2
101	1	1	0	6434.1747	0.5	3
101	2	0	2	6447.5562	0.5	3
101	2	1	2	6458.9125	1.0	1
101	2	1	1	6467.1839	0.5	2
101	2	2	1	6507.6369	0.5	4
101	2	2	0	6507.9669	0.5	2
101	3	0	3	6491.4960	0.2	3
101	3	1	3	6499.9365	0.6	2
101	3	1	2	6516.3986	0.5	2
101	3	2	2	6552.8616	0.4	3
101	3	2	1	6554.6918	1.0	1
101	3	3	1	6625.6806	0.9	2
101	3	3	0	6625.7137	0.6	2
101	4	0	4	6548.5936	0.4	4
101	4	1	4	6554.2377	0.6	2
101	4	1	3	6581.4409	0.2	2
101	4	2	2	6618.0930	0.4	3
101	4	3	2	6686.5599	0.5	2
101	4	3	1	6686.7809	0.4	3

Table 5 (*continued*)

Vib	J	K_a	K_c	E^{OBS}	dE	Nt
101	4	4	1	6785.8152	0.8	2
101	4	4	0	6785.8160	0.8	2
101	5	0	5	6618.1330	1.0	1
101	5	1	5	6621.5824	0.5	2
101	5	1	4	6661.7162	0.4	3
101	5	2	4	6687.4652	0.5	2
101	5	2	3	6698.5429	0.3	3
101	5	3	3	6762.7645	0.3	3
101	5	3	2	6763.6231	0.5	3
101	5	4	2	6861.7203	0.2	2
101	5	4	1	6861.7404	1.0	1
101	5	5	1	6987.3943	1.4	1
101	5	5	0	6987.3944	1.4	1
101	6	0	6	6699.7716	1.0	1
101	6	1	6	6701.7344	0.6	3
101	6	1	5	6756.4347	0.4	4
101	6	2	5	6776.2035	0.4	2
101	6	2	4	6795.9676	0.5	2
101	6	3	4	6854.4034	0.6	2
101	6	3	3	6856.7083	0.3	2
101	6	4	3	6952.9702	1.0	1
101	6	4	2	6953.0717	0.3	2
101	6	5	2	7078.1624	1.0	1
101	6	5	1	7078.1457	1.1	1
101	6	6	1	7229.5649	1.2	1
101	6	6	0	7229.5650	1.1	1
101	7	0	7	6793.4425	0.5	2
101	7	1	7	6794.5053	0.6	3
101	7	1	6	6864.6424	0.5	3
101	7	2	6	6878.7704	1.0	2
101	7	2	5	6909.8974	0.6	2
101	7	3	5	6960.7533	1.0	1
101	7	3	4	6966.5850	0.6	2
101	7	5	3	7184.1721	1.0	1
101	7	6	2	7335.0323	1.3	1
101	7	6	1	7335.0313	1.5	1
101	7	7	1	7511.2950	1.4	1
101	7	7	0	7511.2951	1.4	1
101	8	0	8	6899.2055	0.9	2
101	8	1	7	6985.4364	1.0	1
101	8	3	6	7082.1949	1.1	1
101	9	1	9	7017.3902	1.1	2
101	9	1	8	7118.1518	1.8	1
101	9	2	8	7123.9726	1.6	1
101	9	3	6	7238.2653	1.1	1
101	10	1	10	7147.3215	1.9	1
210	0	0	0	6728.2591	1.1	1
210	1	0	1	6743.2384	0.5	2
210	1	1	1	6760.2628	1.0	1
210	1	1	0	6763.1206	0.2	2
210	2	0	2	6772.8458	0.7	2
210	2	1	2	6787.4258	0.4	3
210	2	1	1	6795.9743	0.3	2
210	2	2	1	6836.9511	1.0	1
210	2	2	0	6837.2738	0.2	2
210	3	0	3	6816.4497	0.6	2
210	3	1	3	6827.9582	1.0	1
210	3	1	2	6845.0469	1.0	1
210	3	2	2	6881.8617	0.3	2
210	3	2	1	6883.4939	1.0	1
210	3	3	1	6969.6877	1.0	1
210	3	3	0	6969.7139	0.7	2
210	4	0	4	6873.2434	1.0	1
210	4	1	3	6910.1052	1.0	1
210	4	2	3	6941.4458	1.0	1
210	4	2	2	6946.1303	0.2	2
210	4	3	1	7029.9949	1.0	1
210	4	4	1	7146.6465	1.2	1
210	4	4	0	7146.6454	1.2	1

Table 5 (continued)

Vib	J	K_a	K_c	E^{OBS}	dE	Nt
210	5	0	5	6942.5188	0.3	3
210	5	1	5	6948.3314	0.3	2
210	5	1	4	6990.8089	1.0	1
210	5	2	4	7015.4321	1.0	1
210	5	2	3	7025.6420	0.2	2
210	5	3	2	7105.7912	0.3	2
210	5	4	2	7221.5794	1.0	1
210	5	5	1	7368.5334	1.2	1
210	5	5	0	7368.5335	1.1	1
210	6	0	6	7023.8673	1.0	1
210	6	1	6	7027.7443	1.0	1
210	6	1	5	7086.9291	1.0	1
210	6	3	4	7195.4771	1.0	1
210	7	0	7	7117.1672	1.0	1
210	7	3	4	7305.5102	1.0	1
210	7	4	3	7417.2009	1.0	1
210	8	2	6	7364.2624	1.0	1
210	8	3	6	7421.0300	1.0	1
210	9	2	8	7449.0536	1.1	1
210	10	1	10	7470.1712	1.2	1

Notations: Vib J K_a K_c—vibrational and rotational quantum numbers; E^{OBS}—experimental value of the energy level (cm^{-1}); dE—the energy levels uncertainties (in units 10^{-3} cm^{-1}); Nt—number of transitions for the energy level determination.

detailed absorption line list can be generated based on precise line positions calculated as a difference between upper and lower experimental energy levels completed by accurate PS intensities. Comparison of experimental absorption lines and those calculated from the experimental energy levels of D_2 ^{18}O is shown in Fig. 6. The impact of the new information on rovibrational energy levels obtained for both HD^{18}O and D_2 ^{18}O molecules is also illustrated in Fig. 7.

4.3. HD^{17}O and D_2 ^{17}O

Assignments of the HD^{17}O and D_2 ^{17}O absorption lines, which are, mostly, among the weakest ones, have been performed at the last stage of our spectrum analysis. The variational calculation [14] of the line positions is essentially worse for the HD^{17}O and D_2 ^{17}O compared to HD^{18}O and D_2 ^{18}O, with the *RMS* deviations of 0.315 and 0.381 cm^{-1}, and maximal deviations of 0.468 and 0.559 cm^{-1}, respectively. Comparison of all experimental and PS energy levels for the HD^{17}O and D_2 ^{17}O isotopologues is presented in Fig. 8. Overall, 296 and 158 new energy levels were derived for HD^{17}O and D_2 ^{17}O, respectively (see Table 4).

Total sets of the obtained energy levels are presented as Supplementary Material II (for all four isotopologues) and included in Tables 5 and 6 (for the HD^{17}O and D_2 ^{17}O isotopologues). New and corrected energy levels corresponding to a previous report for HD^{18}O and D_2 ^{18}O are marked with "NEW ". As one of the main criteria of the spectrum assignment, the deviations from variational calculation [14] are also presented in the tables of Supplementary Material II. Note the special mark "DIS" is given for the energy levels derived from blended lines with less accuracy.

Table 6
New experimental energy levels of the D_2 ^{17}O molecule.

Vib	J	K_a	K_c	E^{OBS}	dE	Nt
031	4	2	3	6382.9546	0.9	1
111	0	0	0	6512.8589	2.7	1
111	1	0	1	6524.7475	1.3	2
111	1	1	1	6533.0737	2.2	1
111	1	1	0	6535.6472	1.4	1
111	2	0	2	6548.0067	2.4	1
111	2	1	2	6554.2938	1.4	1
111	2	1	1	6562.0152	1.5	2
111	2	2	1	6586.8513	0.8	2
111	2	2	0	6587.3561	1.5	2
111	3	0	3	6581.7139	1.0	2
111	3	1	3	6585.8148	1.2	1
111	3	1	2	6601.1635	1.0	2
111	3	2	2	6622.6552	0.9	2
111	3	2	1	6625.0644	0.6	3
111	3	3	1	6670.2887	1.0	2
111	3	3	0	6670.3548	0.9	2
111	4	0	4	6624.9708	1.7	1
111	4	1	4	6627.3828	0.7	3
111	4	1	3	6652.5538	1.2	2
111	4	2	3	6669.9477	0.6	3
111	4	2	2	6676.4636	1.1	2
111	4	3	2	6719.9240	1.0	2
111	4	3	1	6720.2972	1.0	2
111	4	4	1	6783.6371	1.3	1
111	4	4	0	6783.6480	2.1	1
111	5	0	5	6677.3248	1.0	2
111	5	1	5	6678.8308	1.1	2
111	5	1	4	6715.3415	0.9	2
111	5	2	4	6728.4150	1.0	2
111	5	2	3	6741.5646	0.6	3
111	5	3	3	6781.4631	1.1	3
111	5	3	2	6782.7703	0.7	3
111	5	4	2	6843.1800	1.5	2
111	5	4	1	6843.2572	0.9	2
111	5	5	1	6926.3184	2.5	2
111	5	5	0	6926.3187	1.0	2
111	6	0	6	6738.7362	1.7	2
111	6	1	6	6738.3455	1.0	2
111	6	1	5	6788.4739	1.3	3
111	6	2	5	6797.7903	0.9	1
111	6	2	4	6819.8791	1.7	2
111	6	3	4	6854.9092	0.8	2
111	6	3	3	6858.4043	1.8	1
111	6	4	3	6914.9754	1.0	2
111	6	4	2	6915.2885	2.4	2
111	6	5	2	6998.2412	1.1	3
111	6	5	1	6998.2410	2.7	3
111	6	6	1	7097.4659	2.2	1
111	6	6	0	7097.4697	3.8	1
111	7	0	7	6809.2611	1.5	1
111	7	1	7	6809.3624	1.5	1
111	7	1	6	6870.9784	1.2	2
111	7	2	6	6878.4670	1.7	2
111	7	2	5	6910.5729	1.0	2
111	7	3	5	6940.1812	1.5	2
111	7	3	4	6947.7596	1.0	3
111	7	4	4	6999.0545	2.4	1
111	7	4	3	7000.0135	1.1	2
111	7	5	3	7082.4323	2.7	1
111	7	5	2	7082.4112	1.1	2
111	7	6	2	7181.4106	3.1	3
111	7	6	1	7181.4071	1.7	2
111	7	7	1	7295.9656	3.7	1
111	7	7	0	7295.9652	2.7	1
111	8	0	8	6888.9789	2.1	2
111	8	1	8	6889.0292	1.3	2
111	8	1	7	6962.3422	2.2	2
111	8	2	7	6962.9461	1.9	1

Table 6 (*continued*)

Vib	J	K_a	K_c	E^{OBS}	dE	Nt
111	8	2	6	7012.5912	2.2	1
111	8	3	6	7036.5956	1.9	1
111	8	3	5	7050.9976	1.8	1
111	8	4	5	7095.3524	1.2	2
111	8	4	4	7097.8119	2.6	2
111	8	5	4	7179.0232	2.4	1
111	8	6	3	7277.5557	1.6	2
111	8	6	2	7277.5569	3.0	1
111	8	7	2	7391.6666	2.5	1
111	9	0	9	6977.9122	1.8	2
111	9	1	9	6977.9292	2.6	2
111	9	1	8	7062.4137	2.2	1
111	9	2	8	7063.1233	2.6	2
111	9	2	7	7123.9620	1.6	1
111	9	3	6	7167.6444	2.0	1
111	9	4	6	7203.5544	3.0	1
111	9	5	4	7288.1005	1.7	1
111	10	0	10	7076.0419	2.8	2
111	10	1	10	7076.0609	2.4	1
111	10	2	9	7171.8503	2.0	2
111	11	0	11	7183.4105	2.2	1
111	11	1	11	7183.4279	3.2	1
111	11	1	10	7289.5031	2.2	1
111	11	2	10	7289.7019	3.4	1
111	11	2	9	7376.8455	2.5	1
111	12	0	12	7299.9983	3.5	1
111	12	1	12	7300.0021	2.4	1
201	1	0	1	7889.9726	1.3	2
201	1	1	0	7899.5611	1.4	1
201	2	0	2	7912.8999	2.4	1
201	2	1	2	7918.2525	1.0	3
201	2	2	1	7946.8526	0.8	2
201	2	2	0	7947.3704	2.6	1
201	3	0	3	7946.0931	1.6	1
201	3	1	2	7964.0010	1.0	2
201	3	2	1	7986.1600	0.9	2
201	3	3	1	8023.8604	1.5	1
201	3	3	0	8023.9310	0.9	2
201	4	0	4	7988.7118	1.7	1
201	4	1	4	7988.7809	1.0	1
201	4	1	3	8014.4241	1.2	2
201	4	2	3	8025.6259	0.7	2
201	4	2	2	8036.8612	1.2	1
201	4	3	2	8070.7747	0.8	2
201	4	4	1	8128.5149	1.2	1
201	4	4	0	8128.5081	2.0	1
201	5	0	5	8040.3527	0.9	3
201	5	1	5	8040.7739	1.3	1
201	5	1	4	8075.9118	1.0	2
201	5	2	4	8083.0897	1.4	1
201	5	2	3	8100.6642	0.7	2
201	5	3	3	8129.5952	1.2	2
201	5	3	2	8131.3305	0.9	2
201	5	4	1	8187.5220	0.9	2
201	5	5	1	8260.4921	2.7	1
201	5	5	0	8260.4918	1.3	1
201	6	0	6	8101.0497	1.7	2
201	6	1	6	8101.2419	1.0	2
201	6	2	4	8177.2892	2.2	1
201	6	3	4	8200.2189	1.3	1
201	6	4	3	8258.4956	1.3	1
201	6	4	2	8258.8966	2.4	1
201	6	5	2	8331.3751	1.4	1
201	6	5	1	8331.2697	2.7	1
201	7	0	7	8170.8777	1.3	2
201	7	1	7	8170.9491	1.5	1
201	7	1	6	8228.0536	1.6	1
201	7	2	5	8265.9486	1.2	1
201	8	1	8	8249.9079	1.3	2

Table 6 (*continued*)

Vib	J	K_a	K_c	E^{OBS}	dE	Nt
201	8	2	7	8318.4330	1.7	1
201	9	0	9	8338.0806	1.8	2
201	9	1	9	8338.0966	2.6	2
201	10	1	10	8435.5040	1.8	1
201	10	3	8	8597.3321	1.9	1
201	11	0	11	8542.1038	2.2	1
201	11	1	10	8639.0894	2.2	1
201	12	0	12	8657.7987	3.5	1
201	12	1	12	8657.8025	2.4	1
210	4	4	1	6711.8803	1.0	2
210	4	4	0	6711.8177	0.9	2
210	5	4	2	6771.3888	0.8	2
210	5	4	1	6771.0661	1.2	2
210	6	2	4	6744.1199	1.0	1
210	6	4	3	6843.6181	1.7	1
210	6	4	2	6842.7370	0.8	2
210	7	1	7	6733.3166	1.5	1
210	7	4	3	6926.8612	1.7	2
300	4	2	2	7993.6982	1.0	1
300	5	3	3	8087.9126	1.1	1

Notations: Vib J K_a K_c—vibrational and rotational quantum numbers; E^{OBS}—experimental value of the energy level (cm^{-1}); dE—the energy levels uncertainties (in units 10^{-3} cm^{-1}); Nt—number of transitions for the energy level determination.

Combination differences (CD) provide an additional check of the declared experimental accuracy of line positions. The averaged experimental uncertainty for all energy levels of four considered isotopologues derived from two or more lines (2441 of 3338 levels) was calculated to be on the order of 0.0013 cm^{-1}, and agree with the estimated line center accuracy of 0.0009 cm^{-1} given in Section 2. Then, in the resulting linelist for all transitions included in a CD of two and more lines, we attached the deviation of the observed position from that calculated from the upper and lower experimental energy levels (instead of averaged experimental uncertainty of 0.001 cm^{-1} in all other cases). This information helps to discriminate lines or outliers in the CDs which, most probably, have worse accuracy compared to the averaged value.

5. Conclusion

A high resolution Fourier transform absorption spectrum of water vapor enriched by deuterium and oxygen-18 was recorded and assigned in the 6000–9200 cm^{-1} spectral range. More than 14,000 lines of nine water isotopologues ($H_2 {}^{16}O$, $HD^{16}O$, $D_2 {}^{16}O$, $H_2 {}^{18}O$, $HD^{18}O$, $D_2 {}^{18}O$, $H_2 {}^{17}O$, $HD^{17}O$ and $D_2 {}^{17}O$) were observed and assigned. The spectrum assignment was based on previously reported experimental energy levels as well as on the variational calculations of water spectra. Numerous lines of the $HD^{18}O$, $D_2 {}^{18}O$, $HD^{17}O$ and $D_2 {}^{17}O$ isotopologues were observed for the first time. A large set of 3338 precise consistent experimental energy levels was derived for the isotopologues mentioned above by processing the observed vibration–rotation transitions via RITZ computer code based on the Rydberg–Ritz fundamental principle. 2627 energy levels are reported for the first time.

The new information includes 16 vibrational bands observed for the $HD^{18}O$, $D_2^{18}O$, $HD^{17}O$ and $D_2^{17}O$ isotopologues. Existing information on the energy levels for a number of vibrational states of $HD^{18}O$ molecule was significantly enlarged. In all previous studies the $HD^{18}O$ and $D_2^{18}O$ lines falling in our region were among the weakest ones, as either ^{18}O [5,36] or deuterium [57,58] enriched samples have been used, and never an $^{18}O+D$ enriched sample. That is why we believe our energy levels sets derived from stronger absorption and, consequently, more abundant combination differences are generally more precise than previously reported data. The energy level set obtained in this study, together with accurate variational intensities, can be used for the generation of detailed absorption line lists for the $HD^{18}O$, $D_2^{18}O$, $HD^{17}O$ and $D_2^{17}O$ isotopologues which can have numerous applications.

Though no new upper energy levels have been found for the $HD^{16}O$ and $D_2^{16}O$ isotopologues, 237 lines were observed for the first time.

The accuracy of variational energy levels was found to decrease essentially for the $HD^{17}O$ and $D_2^{17}O$ isotopologues with a *RMS* deviation with the experiment up to 0.38 cm^{-1}. The new information derived in this study will help to optimize the potential energy surfaces of these isotopologues.

Acknowledgments

Appendix A. Supporting information

Supplementary data associated with this article can be found in the online version at doi:10.1016/j.jqsrt.2012.02.009.

References

[1] Zelinger Z, Barret B, Kubát P, Ricaud P, Attie JL, Le Flochmoën E, et al. Observations of $HD^{18}O$, CH_3OH and vibrationally-excited N_2O from Odin/SMR measurements. Mol Phys 2006;104:2815–20.

[2] Bergin EA, Phillips TG, Comito C, Crockett NR, Lis DC, Schilke P, et al. Herschel observations of extra-ordinary sources (HEXOS): the present and future of spectral surveys with Herschel/HIFI. Astron Astrophys 2010;521:L20.

[3] Rothman LS, Gordon IE, Barbe A, Benner DC, Bernath PF, Birk M, et al. The HITRAN 2008 molecular spectroscopic database. J Quant Spectrosc Radiat Transfer 2009;110:533–72.

[4] Jacquinet-Husson N, Crepeau L, Armante R, Boutammine C, Chédin A, Scott NA, et al. The 2009 edition of the GEISA spectroscopic database. J Quant Spectrosc Radiat Transfer 2011;112:2395–445.

[5] Liu AW, Du JH, Song KF, Wang L, Wan L, Hu SM. High-resolution Fourier-transform spectroscopy of ^{18}O enriched water molecule in the 1080–7800 cm^{-1} region. J Mol Spectrosc 2006;237:149–62.

[6] Ni HY, Liu AW, Song KF, Hu SM, Naumenko OV, Kruglova TV, et al. High-resolution spectroscopy of the triple-substituted isotopologue of water $D_2^{18}O$: the first triad. Mol Phys 2008;106:1793–801.

[7] Liu AW, Song KF, Ni HY, Hu SM, Naumenko OV, Vasilenko IA, et al. (000) and (010) energy levels of the $HD^{18}O$ and $D_2^{18}O$ molecules from analysis of their v_2 bands. J Mol Spectrosc 2011;265:26–38.

[8] Nikitin AV, Kochanov RV. Visualization and identification of spectra by the SpectraPlot program. Atmos Ocean Opt 2011;24:936–41 in Russian.

[9] Toth RA. Extensive measurements of $H_2^{16}O$ line frequencies and strengths: 5750 to 7965 cm^{-1}. Appl Opt 1994;33:4851–67.

[10] Tolchenov RN, Tennyson J. Water line parameters for weak lines in the range 7400–9600 cm^{-1}. J Mol Spectrosc 2005;231:23–7.

[11] Toth RA. Transition frequencies and strengths of $H_2^{17}O$ and $H_2^{18}O$: 6600 to 7640 cm^{-1}. Appl Opt 1994;33:4868–79.

[12] Toth RA. Line positions and strengths of HDO between 6000 and 7700 cm^{-1}. J Mol Spectrosc 1997;186:66–89.

[13] Daumont L, Jenouvrier A, Régalia-Jarlot L, Fally S, Carleer M, Hermans C, et al. Fourier transform infrared spectroscopy of H_2O, HDO and D_2O: line parameters in the 5500–10 800 cm^{-1} spectral region. In: 12th colloquium on high-resolution molecular spectroscopy, Dijon, September 3–7, 2007, Poster H4; Daumont L, Mikhailenko S. Private communication (2009).

[14] ⟨http://spectra.iao.ru⟩.

[15] Toth RA, Margolis JS. Line positions of H_2O in the 1.33 to 1.45 µm region. J Mol Spectrosc 1975;55:229–51.

[16] Flaud JM, Camy-Peyret C, Maillard JP, Guelachvili G. Higher ro-vibrational levels of H_2O deduced from high resolution oxygen-hydrogen flame spectra between 6200 and 9100 cm^{-1}. Mol Phys 1977;33:1641–50.

[17] Flaud JM, Camy-Peyret C, Rao KN, Chen DW, Hoh YS, Maillard JP. Spectrum of water vapor between 8050 and 9370 cm^{-1}. J Mol Spectrosc 1979;75:339–62.

[18] Mandin JY, Chevillard JP, Camy-Peyret C, Flaud JM. Line intensities in the v_1+2v_2, $2v_2+v_3$, v_1+v_3, $2v_3$, and $v_1+v_2+v_3-v_2$ bands of $H_2^{16}O$, between 6300 and 7900 cm^{-1}. J Mol Spectrosc 1986;118:96–102.

[19] Mandin JY, Chevillard JP, Flaud JM, Camy-Peyret C. $H_2^{16}O$: line positions and intensities between 8000 and 9500 cm^{-1}: the second hexad of interacting vibrational states {(050), (130), (031), (210), (111), (012)}. Can J Phys 1988;66:997–1011.

[20] Schermaul R, Learner RCM, Newnham DA, Williams RG, Ballard J, Zobov NF, et al. The water vapor spectrum in the region 8600–15000 cm^{-1}: experimental and theoretical studies for a new spectral line database. I. Laboratory measurements. J Mol Spectrosc 2001;208:32–42.

[21] Smith KM, Ptashnik I, Newnham DA, Shine KP. Absorption by water vapour in the 1 to 2 µm region. J Quant Spectrosc Radiat Transfer 2004;83:735–49.

[22] Toth RA. Measurements of positions, strengths and self-broadened widths of H_2O from 2900 to 8000 cm^{-1}: Line strength analysis of the 2nd triad bands. J Quant Spectrosc Radiat Transfer 2005;94:51–107.

[23] Jenouvrier A, Daumont L, Régalia-Jarlot L, VlG Tyuterev, Carleer M, Vandaele AC, et al. Fourier transform measurements of water vapor line parameters in the 4200–6600 cm^{-1} region. J Quant Spectrosc Radiat Transfer 2007;105:326–55.

[24] Mikhailenko SN, Keppler Albert KA, Mellau G, Klee S, Winnewisser BP, Winnewisser M, Tyuterev VIG. Water vapor line intensities in the 1900–6600 cm^{-1} region. J Quant Spectrosc Radiat Transfer 2008;109:2687–96.

[25] Parvitte B, Zeninari V, Pouchet I, Durry G. Diode laser spectroscopy of H_2O in the 7165–7185 cm^{-1} range for atmospheric applications. J Quant Spectrosc Radiat Transfer 2002;75:493–505.

[26] Macko P, Romanini D, Mikhailenko SN, Naumenko OV, Kassi S, Jenouvrier A, et al. High sensitivity CW-cavity ring down spectroscopy of water in the region of the 1.5 µm atmospheric window. J Mol Spectrosc 2004;227:90–108.

[27] Mikhailenko SN, Wang L, Kassi S, Campargue A. Weak water absorption lines around 1.455 and 1.66 μm by CW-CRDS. J Mol Spectrosc 2007;244:170–8.

[28] Liu X, Zhou X, Jeffries JB, Hanson RK. Experimental study of H_2O spectroscopic parameters in the near-IR (6940–7440 cm^{-1}) for gas sensing applications at elevated temperature. J Quant Spectrosc Radiat Transfer 2007;103:565–77.

[29] Lisak D, Havey DK, Hodges JT. Spectroscopic line parameters of water vapor for rotation-vibration transitions near 7180 cm^{-1}. Phys Rev A 2009;79:052507.

[30] Mikhailenko S, Kassi S, Wang L, Campargue A. The absorption spectrum of water in the 1.25 μm transparency window (7408–7920 cm^{-1}). J Mol Spectrosc 2011;269:92–103.

[31] Toth RA, Flaud JM, Camy-Peyret C. Spectrum of $H_2{}^{18}O$ and $H_2{}^{17}O$ in the 6974 to 7387 cm^{-1} region. J Mol Spectrosc 1977;67:206–18.

[32] Chevillard JP, Mandin JY, Flaud JM, Camy-Peyret C. $H_2^{18}O$: the (030), (110), and (011) interacting states. Line positions and intensities for the $3\nu_2$, $\nu_1+\nu_2$, and $\nu_2+\nu_3$ bands. Can J Phys 1985;63:1112–27.

[33] Chevillard JP, Mandin JY, Camy-Peyret C, Flaud JM. The first hexad [(040), (120), (021), (200), (101), (002)] of $H_2^{18}O$: experimental energy levels and line intensities. Can J Phys 1986;64:746–61.

[34] Liu AW, Naumenko O, Song KF, Voronin B, Hu SM. Fourier-transform absorption spectroscopy of $H_2^{18}O$ in the first hexade region. J Mol Spectrosc 2006;236:127–33.

[35] Liu AW, Hu SM, Camy-Peyret C, Mandin JY, Naumenko O, Voronin B. Fourier transform absorption spectra of $H_2{}^{17}O$ and $H_2^{18}O$ in the 8000–9400 cm^{-1} spectral region. J Mol Spectrosc 2006;237:53–62.

[36] Liu A, Naumenko O, Kassi S, Campargue A. High sensitivity CW–CDRS of ^{18}O enriched water near 1.6 μm. J Quant Spectrosc Radiat Transfer 2009;110:1781–800.

[37] Moretti L, Sasso A, Gianfrani L, Ciurylo R. Collisional-broadened and Dicke-narrowed lineshapes of $H_2^{16}O$ and $H_2^{18}O$ transitions at 1.39 μm. J Mol Spectrosc 2001;205:20–7.

[38] Tennyson J, Bernath PF, Brown LR, Campargue A, Carleer MR, Császár AG, et al. IUPAC critical evaluation of the rotational-vibrational spectra of water vapor. Part I. Energy levels and transition wavenumbers for $H_2{}^{17}O$ and $H_2^{18}O$. J Quant Spectrosc Radiat Transfer 2009;110:573–96.

[39] Ulenikov ON, Hu SM, Bekhtereva ES, Onopenko GA, Wang XH, He SG, et al. High-resolution Fourier transform spectrum of HDO in the region 6140–7040 cm^{-1}. J Mol Spectrosc 2001;208:224–35.

[40] Naumenko OV, Voronina S, Hu SM. High resolution Fourier transform spectrum of HDO in the 7500–8200 cm^{-1} region: revisited. J Mol Spectrosc 2004;227:151–7.

[41] Ulenikov ON, Hu SM, Bekhtereva ES, Zhu QS. High-resolution rovibrational spectroscopy of HDO in the region of 8900–9600 cm^{-1}. J Mol Spectrosc 2005;231:57–65.

[42] Oshima T, Sasada H. 1.5-μm DFB semiconductor laser spectroscopy of deuterated water. J Mol Spectrosc 1989;136:250–63.

[43] Naumenko O, Leshchishina O, Campargue A. High sensitivity absorption spectroscopy of HDO by ICLAS–VeCSEL between 9100 and 9640 cm^{-1}. J Mol Spectrosc 2006;236:58–69.

[44] Sasada H, Takeuchi S, Iritani M, Nakatani K. Semiconductor-laser heterodyne frequency measurements of 1.52-μm molecular transitions. J Opt Soc Am B 1991;8:713–8.

[45] Tennyson J, Bernath PF, Brown LR, Campargue A, Császár AG, Daumont L, et al. IUPAC critical evaluation of the rotational–vibrational spectra of water vapor Part II. Energy levels and transition wavenumbers for $HD^{16}O$, $HD^{17}O$, and $HD^{18}O$. J Quant Spectrosc Radiat Transfer 2010;111:2160–84.

[46] Dickey FP, Guderjahn CA, Palik ED. The combination band of $\nu_1+\nu_2+\nu_3$ of heavy water vapour. J Chem Phys 1952;20:375–7.

[47] Benedict WS, Gailar N, Plyler EK. Rotation–vibration spectra of deuterated water vapor. J Chem Phys 1956;24:1139–65.

[48] Ormsby PS, Rao KN, Winnewisser M, Winnewisser BP, Bykov AD, Naumenko OV, et al. The $3\nu_2+\nu_3$, $\nu_1+\nu_2+\nu_3$, $\nu_1+3\nu_2$, $2\nu_1+\nu_2$, and $\nu_2+2\nu_3$ bands of $D_2{}^{16}O$: the second hexade of interacting states. J Mol Spectrosc 1993;158:109–30.

[49] Bykov AD, Naumenko OV, Sinitsa LN, Winnewisser BP, Winnewisser M, Ormsby PS, et al. The hot band $\nu_1+2\nu_2+\nu_3-\nu_2$ of $D_2{}^{16}O$. J Mol Spectrosc 1994;166:169–75.

[50] Cohen Y, Rosenwaks S. Spectroscopy of D_2O (2,0,1). J Mol Spectrosc 1996;180:298–304.

[51] Ulenikov ON, He SG, Onopenko GA, Bekhtereva ES, Wang XH, Hu SM, et al. High-resolution study of the $(\nu_1+\nu_2+\nu_3=3)$ polyad of strongly interacting vibrational bands of D_2O. J Mol Spectrosc 2000;204:216–25.

[52] Zheng JJ, Ulenikov ON, Onopenko GA, Bekhtereva ES, He SG, Wang XH, et al. High-resolution vibration–rotation spectrum of D_2O in the region near the $2\nu_1+\nu_2+\nu_3$ absorption band. Mol Phys 2001;99:931–7.

[53] Bykov AD, Naumenko OV, Polovtseva ER, Hu SM, Liu AW. Fourier transform absorption spectrum of $D_2{}^{16}O$ in 7360–8440 cm^{-1} region. J Quant Spectrosc Radiat Transfer 2010;111:2197–210.

[54] Naumenko OV, Leshchishina O, Shirin S, Jenouvrier A, Fally S, Vandaele AC, et al. Combined analysis of the high sensitivity Fourier transform and ICLAS–VeCSEL absorption spectra of D_2O between 8800 and 9520 cm^{-1}. J Mol Spectrosc 2006;238:79–90.

[55] Shirin SV, Zobov NF, Polyansky OL, Tennyson J, Parekunnel T, Bernath PF. Analysis of hot D_2O emission using spectroscopically determined potentials. J Chem Phys 2004;120:206–10.

[56] Zobov NF, Ovsannikov RI, Shirin SV, Polyansky OL, Tennyson J. Infrared emission spectrum of hot D_2O. J Mol Spectrosc 2006;240:112–9.

[57] Mikhailenko SN, Tashkun SA, Putilova TA, Starikova EN, Daumont L, Jenouvrier A, et al. Critical evaluation of rotation–vibration transitions and an experimental dataset of energy levels of $HD^{18}O$. J Quant Spectrosc Radiat Transfer 2009;110:597–608.

[58] Mikhailenko SN, Tashkun SA, Daumont L, Jenouvrier A, Carleer M, Fally S, et al. Line positions and energy levels of the 18-O substitutions from the HDO/D_2O spectra between 5600 and 8800 cm^{-1}. J Quant Spectrosc Radiat Transfer 2010;111:2185–96.

[59] Bellet J, Lafferty WJ, Steenbeckeliers G. Microwave spectra of $D_2{}^{17}O$ and $D_2{}^{18}O$. J Mol Spectrosc 1973;47:388–402.

[60] Fleming JW, Gibson MJ. Far-infrared absorption spectra of water vapor $H_2^{16}O$ and isotopic modifications. J Mol Spectrosc 1976;62:326–37.

[61] Johns JWC. High-resolution far-infrared (20–350 cm^{-1}) spectra of several species of H_2O. J Opt Soc Am B 1985;2:1340–54.

[62] Di Lonardo G, Fusina L. The ν_2 band of $D_2{}^{18}O$. J Mol Spectrosc 1989;135:250–8.

[63] Toth RA. $D_2{}^{16}O$ and $D_2{}^{18}O$ transition frequencies and strengths in the ν_2 bands. J Mol Spectrosc 1993;162:41–54.

[64] Wang WF, Tan TL, Tan BL, Ong PP. The ν_2 bands of $HD^{18}O$ and $D_2{}^{18}O$: rovibrational constants and additional transitions. J Mol Spectrosc 1996;176:226–8.

[65] Toth RA. Measurements of line positions and strengths of $HD^{18}O$ and $D_2{}^{18}O$ in the 2500–4280 cm^{-1} region. J Mol Struct 2005;742:49–68.

[66] Stevenson MJ, Townes CH. Quadrupole moment of O^{17}. Phys Rev 1957;107:635–7.

[67] Steenbeckeliers G Private communication (July 1971).

[68] Toth RA. $HD^{16}O$, $HD^{18}O$, and $HD^{17}O$ transition frequencies and strengths in the ν_2 bands. J Mol Spectrosc 1993;162:20–40.

[69] Verkhoeven J, Dymanus A, Bluyssen H. Hyperfine structure of $HD^{17}O$ by beam-maser spectroscopy. J Chem Phys 1969;50:3330–8.

[70] Toth RA. HDO and D_2O low pressure, long path spectra in the 600–3100 cm^{-1} region II. D_2O line positions and strengths. J Mol Spectrosc 1999;195:98–122.

[71] Schwenke DW. Variational calculations of rovibrational energy levels and transition intensities for tetratomic molecules. J Phys Chem 1996;100:2867–84.

[72] Schwenke DW. Corrections: variational calculations of rovibrational energy levels and transition intensities for tetratomic molecules. J Phys Chem 1996;100:18884.

[73] Partridge H, Schwenke DW. The determination of an accurate isotope dependent potential energy surface for water from extensive *ab initio* calculations and experimental data. J Chem Phys 1997;106:4618–39.

[74] Schwenke DW, Partridge H. Convergence testing of the analytic representation of an *ab initio* dipole moment function for water: Improved fitting yields improved intensities. J Chem Phys 2000;113:6592–7.

[75] Mikhailenko SN, Tyuterev VlG, Mellau G. (000) and (010) states of $H_2^{18}O$: analysis of rotational transitions in hot emission spectrum in the 400–850 cm^{-1}. J Mol Spectrosc 2003;217:195–211.

[76] Mellau G, Mikhailenko SN, Starikova EN, Tashkun SA, Over H, Tyuterev VlG. Rotational levels of the (000) and (010) states of $D_2{}^{16}O$ from hot emission spectra in the 320-860 cm^{-1} region. J Mol Spectrosc 2004;224:32–60.

[77] Mikhailenko SN, Mellau GCh, Starikova EN, Tashkun SA, Tyuterev VlG. Analysis of the first triad of interacting states (020), (100), and (001) of $D_2{}^{16}O$ from hot emission spectra. J Mol Spectrosc 2005;233:32–59.

[78] Naumenko O, Campargue A. High-order resonance interactions in HDO: analysis of the absorption spectrum in the 14980–15350 cm^{-1} spectral region. J Mol Spectrosc 2000;199:59–72.